Composition Control in Emulsion Copolymerization. II. Application to Binary and Ternary Systems

STEFANO CANEGALLO,[1] PAOLO CANU,[1] MASSIMO MORBIDELLI,[1,*] and GIUSEPPE STORTI[2]

[1]Dipartimento di Chimica Fisica Applicata, Politecnico di Milano, Piazza Leonardo da Vinci 32, 20133 Milano, Italy; and [2]Dipartimento di Chimica Inorganica, Metallorganica ed Analitica, Università degli Studi di Padova, Via Marzolo, 1, 35131 Padova, Italy

SYNOPSIS

The optimal monomer feed policy for producing in a semibatch reactor a given amount of polymer with constant instantaneous composition, in the minimum reaction time and complete monomer depletion, as developed in Part I of this work, has been implemented experimentally. Conversion has been monitored on-line using a densitometer suitably connected to the laboratory reactor. The procedure has been applied to two binary and one ternary systems. The composition of the polymer produced has been characterized through various experimental techniques. The composition control procedure is insensitive to most types of irreproducibilities that arise in batch reactions performed in industrial appli-fjcations. © 1994 John Wiley & Sons, Inc.

INTRODUCTION

In the first part of this study,[1] a procedure for evaluating optimal monomer feed policies which allow the production of a given amount of polymer with constant instantaneous composition, in the minimum reaction time and complete monomer depletion, was described. The procedure applies to any number of monomer species and are based on a simple model which predicts the system evolution with respect to conversion instead of time. This approach allows us to avoid the calculation of variables such as the number of particles and the average number of active chains per particle, whose estimation often constitutes the bottle-neck in emulsion polymerization modeling.[2,3] The model requires in fact only the knowledge of the monomer reactivity ratios and of the interphase partition laws. On the other hand, these advantages are counterbalanced by a major requirement for the practical implementation of the calculated feed policies: the need of a reliable on-line monitoring of the evolutionary coordinate, i.e., the polymer conversion.

The availability of on-line sensors for measuring conversion in emulsion polymerization reactors is continuously increasing. Extensive reviews of available instrumentation may be found in the literature.[4,5] Among various alternatives, we selected the densimetric technique, originally developed for homopolymerization systems[6] and subsequently extended to copolymerization systems.[7] More than forty data per minute are obtained, thus resulting in a practically continuous monitoring of the polymer formation.

In this study, we combine the theoretical approach to composition control developed[1] with the on-line monitoring of conversion provided by a densitometer.[7] Our final aim is to validate the predicted optimal open-loop monomer feed policies in the case of both binary and ternary systems. In particular, we have examined the binary copolymerization of methylmethacrylate (MMA) and vinylacetate (VAC) and of styrene (STY) and butylacrylate (BUA), as well as the ternary polymerization of MMA, VAC, and BUA. In all cases, a batch reaction would result in a significant compositional drift, thus asking for accurate composition control.

* To whom correspondence should be addressed.

Journal of Applied Polymer Science, Vol. 54, 1919–1935 (1994)
 CCC 0021-8995/94/121919-17

EXPERIMENTAL

Experimental Apparatus

The polymerization reactions were carried out in the fully automatized reactor Arrhenius I (Istituto Guido Donegani, ENICHEM Group). The monomer conversion was monitored on-line from the density measurements as provided by a DMA40 digital densitometer (Anton Paar) connected to the reactor with a sampling circuit designed so as to avoid the presence of gas bubbles and the coalescence of monomer droplets. All feed and sample circuits in the reactor were assembled using PTFE tubes. Further details about the reactor and the densitometer, together with a scheme of the apparatus, are reported elsewhere.[7]

It should be noted that because of the small quantity of polymer produced in each experimental run (about 100 g), the composition control policy involves the addition of rather small monomer amounts, thus asking for high precision in the addition procedure. In this study, monomer additions as a function of polymer mass produced have been performed through a computer driven peristaltic pump (4 rolls, Masterflex, Cole Parmer Inst.) equipped with silicone tubes of high-precision internal diameter (I.D. = 0.8 mm). The tubes were externally covered by fluorinated grease, so as to reduce friction and monomer evaporation. After saturation of the silicone tubing with the monomer to be charged to the reactor, the pump was calibrated with this same component just before each reaction by evaluating the number of revolutions needed to produce the overall addition amount desired. A correction accounting for monomer evaporation was also accounted for. Both the densitometer and the peristaltic pump were connected to the serial communication ports of a personal computer.

Commercial monomers (Fluka, RPE grade), contacted with inhibitor remover disposable columns (Aldrich) just before reaction, were used. Water was deionized and distilled, while emulsifier (sodium lauryl sulphate, SLS) and initiator (potassium persulphate, KPS) were used without further purification.

Before ending this section, we will discuss some additional details relative to the procedures of densitometer calibration and monomer addition, which are relevant in performing the experimental runs with composition control described next.

Densitometer Calibration

In the instrument under examination, density ρ is measured through the period of oscillation T of a suitable capillary U-tube. These are related through the equation:

$$\rho = AT^2 + B, \tag{1}$$

where the two constants A and B are instrument calibration parameters. A relative calibration procedure for evaluating these parameters has been developed, based on the results of a preliminary calibration reaction batch. In particular, this provides the difference between the square of the final and initial values of the period of oscillation, i.e., $\Delta T^2 = T_f^2 - T_0^2$, values, i.e., $\Delta\rho = \rho_f - \rho_0$, as obtained by off-line gravimetry. The evaluation of the two calibration constants is then performed through the following equations:

$$A = \frac{\Delta\rho}{\Delta T^2}; \quad B = \rho_0 - AT_0^2 \tag{2}$$

It should be noted that a significant improvement in the calibration procedure is obtained by using in the second of eqs. (2) for evaluating B the density and oscillation period values measured at the beginning of the reaction to be monitored, rather than those measured in the calibration reaction batch. This approach increases the accuracy of the on-line monitoring at low conversion values, where, due to the small amount of copolymer produced, the negative effect of inaccurate monomer additions is more significant. This relative calibration has been adopted for each semibatch reaction discussed in the following, using the corresponding batch reaction (i.e., that with the same cumulative composition) as calibration reaction.

The amount of polymer produced has been estimated from the emulsion density values, ρ_{em} measured on-line, using the following equation based on the volume additivity rule:

$$\frac{1}{\rho_{em}} = v_{em} = \sum_{i=1}^{N_s} W_i v_i \tag{3}$$

In the relation above W_i indicates the overall weight fraction of component i inside the reactor and, independently of the phase in which it is located (aqueous, oil droplets, or polymer particles), v_i its specific volume; N_s is the number of involved components (i.e., monomer species, polymer, water, emulsifier, and initiator).

In the case of batch reactions, eq. (3) reduces to:

$$v_{em} = v_{em}^0 - M_c \frac{\sum_{i=1}^{N_m} Y_i(M_c)\,\Delta v_i}{\sum_{i=1}^{N_s} \hat{M}_i^0} \tag{4}$$

where v_{em}^0 represents the emulsion specific volume at zero conversion, Δv_i ($= v_{mi} - v_{hi}$) the difference between the specific volume of component i in the form of monomer and homopolymer, $Y_i(M_c)$ the weight fraction of the i-th monomer in copolymer when the overall amount of copolymer produced is M_c, $\hat{M}_i^0$ the amount initially charged to the reactor and N_m the number of monomer species. Note that the copolymer composition $Y_i(M_c)$ is estimated on-line using the simple composition-conversion model described in Part I of this work.

In the case of semibatch reactions, the relation between emulsion density and polymer produced becomes more complicated, since the overall amount of reactants in the reactor changes continuously. Let us assume that the monomer additions are discrete in time (see next subsection). Thus, indicating with the superscript n the variable value after the n-th monomer addition and applying eq. (4) between two successive monomer additions, rather than in the entire reaction interval, we obtain:

$$v_{em}^{n+1} = v_{em}^n - M_c \frac{\sum_{i=1}^{N_m} Y_i(M_c)\,\Delta v_i}{\sum_{i=1}^{N_s} \hat{M}_i^n} \tag{5}$$

where $\hat{M}_i^n$ indicates the amount of the i-th monomer charged to the reactor from the beginning up to the last performed addition. The use of eq. (5) requires the knowledge of the adopted addition policy so as to properly update the overall amounts of residual monomer species. It is worth noting in passing that, in the case of constant composition copolymers (as is the case when composition control is successful), the relationship between the emulsion-specific volume and the amount of copolymer produced becomes linear.

Monomer Feed Procedure

The optimal feed policies, provided by the procedure described in Part I of this work as continuous functions of conversion, $\hat{Q}_i(M_c)$, have been implemented in the experimental runs as discrete additions every $\Delta M_c = 2$ g of polymer produced. Thus, starting from $M_c = \Delta M_c$ and up to $M_c = M_c^f - \Delta M_c$, an amount of each monomer species equal to:

$$\Delta\hat{M}_i(M_c^n) = \int_{M_c^n - \Delta M_c/2}^{M_c^n + \Delta M_c/2} \hat{Q}_i dM_c \tag{6}$$

has been charged to the reactor at $M_c^n = n\Delta M_c$. Note that the residual amounts of monomer species corresponding to the first and the last half-intervals (i.e., from 0 to $\Delta M_c/2$ and from $M_c^f - \Delta M_c/2$ to M_c^f) have been added to the initial and to the last addition, respectively.

The discretized feed mode has been preferred over the continuous one since it increases the precision of the monomer additions in our laboratory set-up. The monomer flowrate values required by the composition control were in fact very close to the minimum operating flowrate of the pump, and, therefore, we used larger flowrates but discretized into very short addition time intervals. This difficulty does not arise in larger scale reactors, such as those used in applications.

On the other hand, the discretization of the monomer feed produces some oscillations in the instantaneous copolymer composition. Thus, before implementing this feed procedure, some parametric calculations have been performed so as to determine the instantaneous compositional drift produced by the adopted discretization and the behavior of the corresponding cumulated composition. The results of these preliminary simulations are summarized in Figure 1 with reference to the binary system MMA–VAC and copolymer composition $Y_{MMA} = 0.3$. The monomer addition process has been discretized at three different levels, i.e., every 5, 2, and 0.5 g of polymer produced. The calculated values of the polymer composition, both instantaneous and cumulated, are shown in Figure 1 (a and b), respectively. It is seen that significant oscillations of instantaneous composition may arise when the monomer feed is discretized, due to the different reactivities of the involved monomer species. When reducing the number of monomer additions, the frequency of these oscillations decreases while their amplitude increases. Moreover, whatever the examined discretization levels, the amplitude of the calculated oscillations increases at increasing conversion values. This is so because the amount of monomer species buffered in the latex decreases, and, therefore, the change in monomer composition induced by a fixed amount of polymer produced, increases. In conclusion, we see that the discretization selected (i.e., $\Delta M_c = 2$ g) is satisfactory since it produces reasonable oscillations in the instantaneous

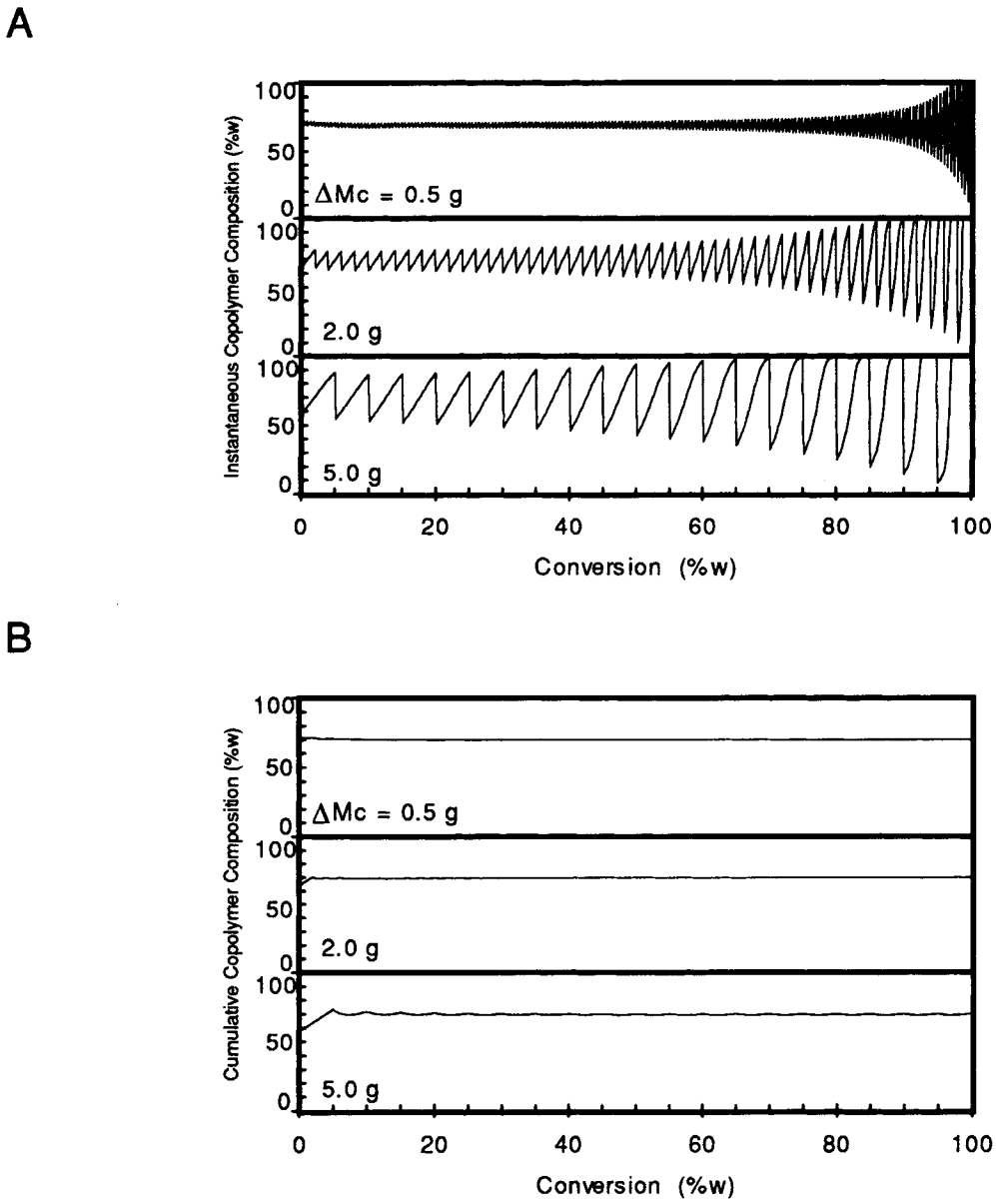

Figure 1 Calculated instantaneous (a) and cumulated (b) copolymer composition as a function of conversion for three different discretization levels of the monomer feed flowrate.

polymer composition, which leads to a practically constant cumulated composition. Note that the results discussed above refer to the system with the maximum difference of monomer reactivities among those considered in this study. Thus, this conclusion holds true for all the examined systems.

Finally, it is worth mentioning that the calculated initial amounts of the monomer species also have to be charged with particular accuracy, so as to start the copolymer composition at the right value. For this reason, in this study the nitrogen stripping of the initially charged mixture for removing dissolved oxygen has been performed before charging the monomer species. This procedure allows us to avoid the compositional drift of the initial monomer mixture due to selective monomer evaporation.

Polymer Characterization

To check the quality of the polymer produced using the composition-control procedure, several characterization techniques have been used. Some of these

require the extraction of the polymer from a given latex sample. This is done by precipitating the polymer particles with excess methanol 3 times. The final solid recovered may be considered free of residual of monomers and emulsifier.

Densimetry

From a comparison between conversion values estimated by densimetry (on-line) and by gravimetry (off-line), an indirect check of whether or not the polymer composition has been kept constant during the reaction can be obtained. The reason is that, while the gravimetric technique is independent of the polymer composition, the density of the emulsion depends on the composition of both the residual monomer mixture and the copolymer.[7] Thus, a compositional drift results in a continuously increasing deviation between the conversion values estimated by the two techniques.

Gas Chromatography (GC)

The copolymer composition can be estimated from the composition of the residual monomer mixture using simple material balances. The overall amount of each monomer species in the reacting system has been measured off-line by GC of the latex samples collected at various times. A gas chromatograph equipped with a chromosorb w/diethylene glycol succinate packed column has been used, operating at pressure of 80 kPa of carrier gas (nitrogen) and temperatures of 180, 80, and 200°C for injector, column, and detector, respectively. The gas chromatograph was equipped with a FID detector and the reproducibility of the measured concentration values was estimated as ± 1.5% by weight.

Thermal Characterizations

Information about polymer composition can be obtained through thermogravimetric analysis (TGA) as well as from the values of the glass transition temperature, T_g, estimated through differential-scanning calorimetry (DSC). Both these techniques have been used to characterize some of the copolymers produced in this study; we will come back to this point in the last section.

OPTIMAL MONOMER FEED POLICY

Before considering the experimental results, it is useful to summarize the operating procedure and the relevant equations used to predict the optimal monomer feed flowrates to the semibatch reactor. The derivation of the adopted equations is discussed in detail in Part I of this work, while the meaning of each variable is reported in the Nomenclature.

Model Parameters

As mentioned above, the theoretical procedure requires, besides some physical properties of the monomer species and of the polymer, the reactivity ratios and the interphase monomer partition laws. In most cases of practical interest, a reasonable estimate of all these parameters can be found in the literature, and this is indeed the case for the monomer species examined in this study, whose relevant parameter values are summarized in Table I. In particular, note that the linear, oversimplified inter-

Table I Numerical Values of the Model Parameters and Corresponding Literature Sources (1 = STY; 2 = BUA; 3 = MMA; 4 = VAC)

Parameter	Numerical Value	Source (Ref. No.)
Reactivity ratios		
r_{12}	0.70	8
r_{21}	0.20	8
r_{34}	26.00	8
r_{43}	0.03	8
r_{23}	0.12	8
r_{32}	2.86	8
r_{24}	3.48	8
r_{12}	0.02	8
Monomer concentrations in aqueous phase at saturation		
$(M)_1^{w,*}$	$3.65 \cdot 10^{-3}$ mol L^{-1}	9
$(M)_2^{w,*}$	$7.86 \cdot 10^{-2}$ mol L^{-1}	9
$(M)_3^{w,*}$	$1.60 \cdot 10^{-1}$ mol L^{-1}	9
$(M)_4^{w,*}$	$2.79 \cdot 10^{-1}$ mol L^{-1}	9
Monomer densities		
ρ_1	0.88 g cm^{-3}	8
ρ_2	0.86 g cm^{-3}	8
ρ_3	0.91 g cm^{-3}	8
ρ_4	0.94 g cm^{-3}	8
Copolymer density (average value)		
ρ_c	1.10 g cm^{-3}	8
Monomer concentrations in particles at saturation (volume fraction)		
ϕ_1^*	0.60	9
ϕ_2^*	0.60	9
ϕ_3^*	0.71	9
ϕ_4^*	0.85	9

phase partitioning laws described in Ref. 1 have been used.

From the parameter values above, the polymer-free volume fraction of each monomer species in the particles, i.e., $C_i = \phi_i / \phi$ can be evaluated as a function of the desired copolymer composition, Y_i. This is the dual problem of the classical equations by Mayo and Lewis,[10] extended to systems involving any number of monomer species, i.e., to evaluate the monomer mixture composition needed to produce a copolymer with given composition. This problem can be solved numerically in the general case or analytically for a binary system, as illustrated in the Appendix to ref. 1.

Critical Monomer

As *critical monomer* we indicate the component which is entirely charged at the beginning of the reaction and not feed subsequently. All the other monomer species are fed to the reactor during the polymerization. As discussed in the Introduction, the critical monomer can be selected, in terms of desired polymer composition and monomer reactivities, as the component exhibiting the minimum value of the parameter $A_i = Y_i \rho_c / C_i \rho_i$. Actually, this criterion is valid as long as oil droplets are present in the system. Once these disappear, a change in the critical monomer may occur. However, this change does not occur for the systems examined in this work, which are characterized by strongly different reactivities and minor differences in water solubilities (MMA–VAC) or by slightly different reactivities and scarce water solubilities (BUA–STY). This result can be confirmed rigorously through the evaluation of the parameters γ_j following the procedure described in Part I of this work.

Reaction Intervals

The requirements of minimum reaction time and complete monomer depletion lead naturally to divide the reaction in two distinct intervals. In the first one (flooded) droplets are present and polymer particles are saturated by the monomer mixture, i.e., $\phi = \phi^*$. In the second interval (starved), the oil droplets are no longer present and the monomer volume fraction in the polymer particles, ϕ decreases from the saturation value to zero. The transition from the flooded to the starved interval occurs when the amount of polymer produced is equal to the specific value[1]:

$$M_c^* = \frac{M_c^f A_j - B_j \phi^*}{A_j + \dfrac{\phi^*}{1-\phi^*}} \tag{7}$$

where the index j refers to the critical monomer and B_j ($= M_j^{w,*} \phi_c / \phi^* \rho_j$) is a parameter related to the monomer water solubility. The value of M_c^* given by eq. (7) may be negative, as for example when the critical monomer is largely soluble in the aqueous phase, i.e., large values of B_j. In this case, the reaction does not exhibit a flooded interval, but it operates in the starved interval right from the beginning, thus starting from an initial value of the monomer volumetric fraction in the polymer particles lower than the saturation value ϕ^*.

Monomer Feed Flowrates

We now proceed to evaluate the flowrates of non-critical monomers ($i = 1, N_m$; $i \neq j$). The following equations are used, depending on whether the reactor operates in the flooded or in the starved intervals[1]:

- flooded interval

$$\hat{Q}_i(M_c) = \hat{Q}_i^f = \frac{Y_i}{A_i}(A_i - A_j) = \text{constant} \tag{8}$$

- starved interval

$$\hat{Q}_i(M_c) = \hat{Q}_i^s = \frac{Y_i}{A_i}(B_i + w)(\gamma_i - \gamma_j) \tag{9}$$

where the parameter γ_i is evaluated as:

$$\gamma_i = \frac{A_i + z}{B_i + w} \tag{10}$$

and the auxiliary variables $w = M_c/(1 - \phi)^2$ and $z = \phi/(1 - \phi)$ have been introduced for the sake of brevity. The value of the monomer swelling ratio ϕ as a function of the amount of polymer produced, M_c is obtained by solving the material balance of the critical monomer[1]:

$$\phi = \frac{D_j - (D_j + 4B_j M_c)^{1/2}}{2B_j} \tag{11}$$

$$D_j = A_j(M_c^f - M_c) + M_c + B_j \tag{12}$$

Note that the flowrates in eq. (8), corresponding to the flooded interval and expressed as amount of monomer fed per unit mass of copolymer produced, remain constant during the polymerization reaction.

Monomer Initial Amounts

Since the critical monomer is fully charged to the reactor at the beginning of the reaction, the amount of this monomer initially charged is related to the

desired polymer amount and composition, i.e., $\hat{M}_j^0 = M_c^f Y_j$. About the remaining monomer species, the initial amount of each of them must be such that the initial instantaneous composition of the polymer is at the desired value. In other words, we have to charge to the reactor an amount of monomer i such that its equilibrium partitioning between oil droplets and aqueous phase produces composition values compatible with the desired polymer composition. In particular, we need to have the monomer composition in the polymer particles equal to the C_i values computed above in the first step of this procedure. Recalling the linear interphase partition laws,[1] we see that the composition in the oil droplets is given by C_i, while the concentration in the aqueous phase for each monomer is given by the corresponding saturation value multiplied by C_i. Thus, the initial amount of the generic noncritical monomer i can be evaluated through the following material balance:

$$\hat{M}_i^0 = (V_d^0 \rho_i + M_i^{w,*}) C_i \quad i = 1, N_m; \quad i \neq j \qquad (13)$$

where the initial volume of oil droplets, V_d^0 is obtained from the material balance of the critical monomer as:

$$V_d^0 = \frac{\hat{M}_j^0 - C_j M_j^{w,*}}{\rho_j C_j} \qquad (14)$$

Note that when the reactor operates in the starved interval right from the beginning of the reaction (i.e., $A_j M_c^f < B_j \phi^*$ in eq. (7)), we have $V_d^0 = 0$ in eqs. (13), while eq. (14) becomes meaningless since it would imply $V_d^0 < 0$.

COMPARISON WITH EXPERIMENTAL DATA

In this section, we illustrate the application of the optimal monomer feed policy to three different polymerization systems.

Binary System MMA–VAC

From the values of the reactivity ratios reported in Table I, a significant compositional drift is expected when MMA and VAC are copolymerized in a batch reactor. For example, since MMA is much more reactive than VAC, when a copolymer containing a low amount of MMA is desired, the monomer mixture in the reaction locus should be constituted by almost pure VAC. This system is indeed challenging for checking the performance of the developed composition-control procedure. In particular, we consider the case where a copolymer with constant weight fraction of MMA equal to 0.3 is desired; note that the same copolymer but with $Y_{MMA} = 0.7$ was examined elsewhere.

Two experimental runs have been performed, one in the batch mode (run 56) and the other in the semibatch mode by feeding the monomers according to the optimal policy for composition control (run 62). The recipes adopted in the two experiments are reported in Table II, while the values of the model parameters are summarized in Table I. Following the procedure outlined in the previous section, with reference to the production of $M_c^f = 100$ g of polymer, the key parameters in determining the optimal feed policy have been estimated as follows:

	MMA	VAC
Y_i (−)	0.30	0.70
A_i (−)	27.41	0.88
B_i (g)	23.93	37.11
C_i (−)	0.013	0.987
$\hat{Q}_i^f$ (g/g)	0.290	0
$\hat{Q}_i^s$ (g/g)	0.292 ÷ 0.291	0
M_i^0 (g)	0.85	70.00

As expected, since $A_{VAC} < A_{MMA}$, the critical monomer is VAC. Moreover, using eq. (7), the polymer

Table II Recipes of the Experimental Runs

Run	Water (g)	KPS (g)	SLS (g)	MMA (g)	VAC (g)	STY (g)	BUA (g)
56	1,000	1.5	4	30	70	—	—
62	1,000	1.5	4	[b]	70	—	—
65	1,000	0.5	5	—	—	50	50
71	1,000	0.5	5	—	—	[b]	50
72	800	1.2	8	60	80	—	60
74[a]	800	1.2	8	[b]	80	—	[b]
80	800	1.2	8	[b]	80	—	[b]

[a] 1 g $NaHCO_3$ is charged initially to the reactor.
[b] Semibatch run with composition control. The corresponding monomer feed flowrates are reported in the text.

amount corresponding to the transition from flooded to starved interval can be evaluated as $M_c^* = 11.9$ g.

From the results reported above, it can be seen that the flowrate of MMA, $\hat{Q}_{MMA}$ in the flooded interval, given by eq. (8), is constant, while in the starved interval it varies slightly, according to eq. (9). Moreover, we may note that the numerical values of $\hat{Q}_{MMA}$ in the flooded and in the starved interval are very similar and close to the desired copolymer composition, i.e., $Y_{MMA} = 0.3$. This result can be understood by rearranging eq. (9) and using eqs. (8) and (10) to yield:

$$\hat{Q}^s_{MMA} = \frac{Y_{MMA}}{A_{MMA}}\left[(A_{MMA} - A_{VAC}) + (B_{VAC} - B_{MMA})\frac{A_{VAC} + z}{B_{VAC} + w}\right] = \hat{Q}^f_{MMA} + \frac{Y_{MMA}}{A_{MMA}}(B_{VAC} - B_{MMA})\frac{A_{VAC} + z}{B_{VAC} + w} \quad (15)$$

Since in this case the monomer reactivities are largely different (i.e., $Y_{MMA}/A_{MMA} \ll 1$), eq. (15) leads to $\hat{Q}^s_{MMA} \simeq \hat{Q}^f_{MMA}$, thus confirming the values of the flowrates obtained above. Moreover, since $A_{MMA} \gg A_{VAC}$, from eq. (8) we see that $\hat{Q}^f_{MMA}$ closely approaches the desired copolymer composition, Y_{MMA}. In other words, in this case the composition-control imposes that the amount of the noncritical monomer charged to the reactor is completely depleted by the reaction, which implies that the composition in the reaction locus is close to almost pure critical monomer (i.e., $C_{VAC} \simeq 1$).

In Figure 2, the conversion values as estimated by on-line densimetry and by off-line gravimetry are shown as a function of time. The reasonable agreement between the two sets of data confirms the reliability of the on-line estimate of conversion by the densitometer, which can then be used safely to implement the composition-control monomer feed policy. Moreover, the substantially constant rate of polymerization obtained in the semibatch experiment (run 62), as opposed to that obtained in the batch experiment (run 56), is a first qualitative evidence of a constant composition of the monomer mixture in the reaction locus. From the results shown in Figure 2, we also see that the polymerization reaction does not reach 100% of conversion. This is due to the strongly decreased mobility of the growing radical chains at high conversion, which leads to a limiting conversion value equal to about

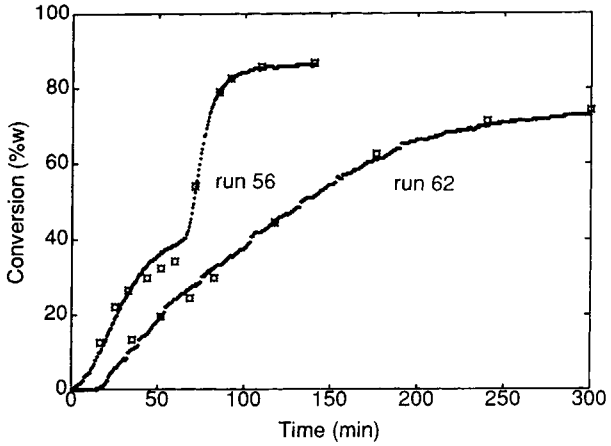

Figure 2 Conversion vs. time curves for runs 56 and 62; densimetric data (●); gravimetric data (□).

90% for the batch reaction (run 56) and 70% for the semibatch reaction (run 62).

In Figure 3, the amount of MMA fed to the reactor in the experimental run 62 is shown as a function of time (a) and conversion (b). While the second diagram exhibits the expected linear behavior, corresponding to $\hat{Q}_{MMA} \simeq 0.3$ g/g, the time evolution is more complex. We note that, as mentioned above, since the polymerization reaction practically stops in the experimental run 62 at a conversion of about 70%, the monomer addition procedure also stops when about 21 g MMA have been charged to the reactor. At this point reacted 70% of the 30 g MMA needed to produce 100 g of polymer with the desired composition.

In Figure 4, the polymer composition as calculated by the same composition–conversion model used in evaluating the monomer feed policies[1] is shown as a function of conversion. These calculated values are believed to closely approach the true composition values, due to the strong validation that this model has received by comparison with a large set of experimental data.[12] Note that in these calculations, the actual monomer addition rather than the theoretical feed policies [i.e., the points instead of the curve in Fig. 3(b)] have been used. The outcome of the monomer feed policy adopted in the semibatch reaction (run 62) is evident, especially when compared with the large compositional drift exhibited by the same reaction performed in the batch mode (run 56).

Finally, in Figure 5, the overall composition of the monomer mixture in the reactor is shown as a function of conversion. Similarly to the previous figure, the curves represent calculated values. How-

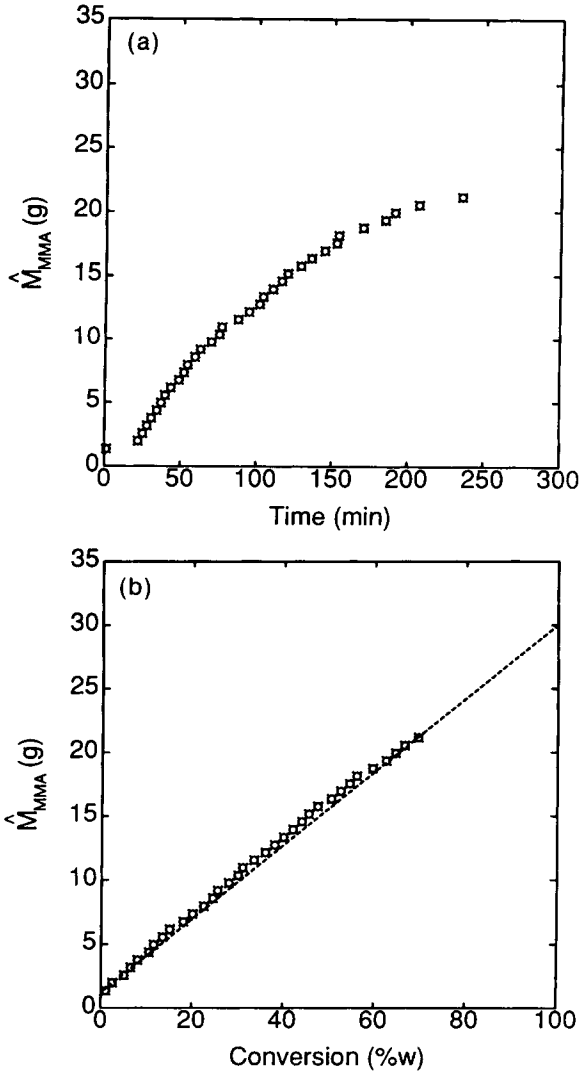

Figure 3 Amount of MMA charged to the reactor in run 62 as a function of time (a) and conversion (b); experimental data (¤); calculated values (- - -).

ever, in this case, experimental data measured by gas-chromatography were available for the batch reaction (run 56). For the semibatch reaction (run 62), the measured values of the weight fraction of VAC in the overall monomer mixture were never significantly different from one. The good agreement between experimental and calculated values constituted a further check of the reliability of the adopted model with respect to the simulation of the composition–conversion relation. We noted again that the effect of the monomer additions was evident, and a practically constant monomer mixture composition was obtained. The oscillations exhibited by the composition curve in the case of semibatch reaction are related to the monomer feed discretization, as discussed earlier in the context of Figure 1.

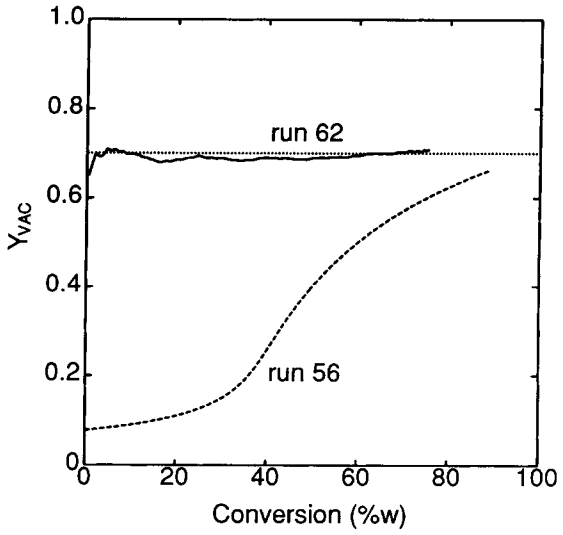

Figure 4 Calculated VAC weight fraction in copolymer, Y_{VAC} as a function of conversion; run 56 (- - -); run 62 (—); desired composition (· · ·).

Binary System BUA–STY

From the data reported in Table I, we see that, with respect to the previous monomer pair, the monomers butylacrylate (BUA) and styrene (STY) are characterized by slightly different reactivities but largely different water solubilities. Also, in this case, two

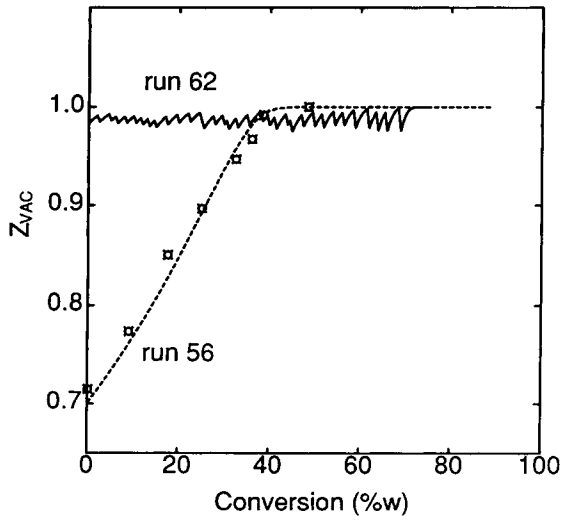

Figure 5 Overall composition of the monomer mixture in the reactor, Z_{VAC}, as a function of conversion. Experimental data: run 56 (¤). Calculated curves: run 56 (- - -); run 62 (—).

experiments are considered: one performed in the batch mode (run 65) and one in the semibatch mode using the optimal monomer feed policy (run 71). The recipes used in the two experimental runs are reported in Table II, while the adopted values of the model parameters are summarized in Table I. Again using the procedure outlined above, the following monomer feed policy has been calculated, with reference to a final polymer production equal to M_c^f = 100 g:

	BUA	STY
Y_i (−)	0.50	0.50
A_i (−)	1.033	1.640
B_i (g)	21.31	0.792
C_i (−)	0.619	0.381
$\hat{Q}_i^f$ (g/g)	0	0.185
$\hat{Q}_i^s$ (g/g)	0	0.249 ÷ 0.239
M_i^0 (g)	50.00	27.76

The copolymer amount corresponding to the transition from flooded to starved interval is M_c^* = 35.8 g. It can be seen that $A_{BUA} < A_{STY}$, thus indicating that BUA is the critical monomer; while $B_{BUA} \gg B_{STY}$ due to the largely different water solubilities of the two monomers. From this, and using eq. (8), we readily see that in this case, the monomer feed in the flooded interval is smaller than the desired copolymer composition, i.e., $\hat{Q}_{STY}^f < Y_{STY}$. Moreover, from eq. (15) we expect an increase in the monomer flowrate when passing from the flooded to the starved interval, which implies $\hat{Q}_{STY}^f < \hat{Q}_{STY}^s$, in agreement with the results reported above. On physical ground, this can be explained by considering that, once the oil droplets disappear, a large amount of critical monomer, buffered in the aqueous phase, becomes available to the polymerization reaction.

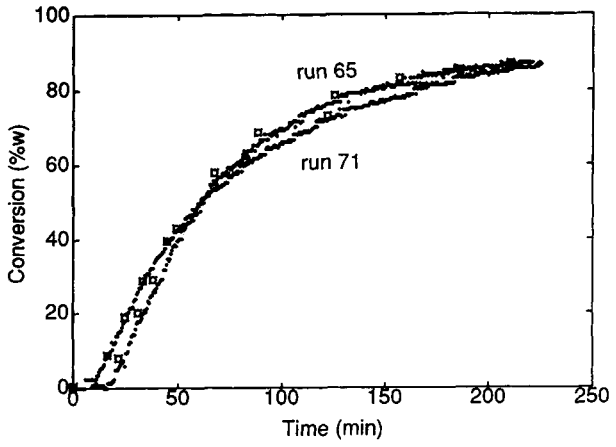

Figure 6 Conversion vs. time curves for runs 65 and 71; densimetric data (●); gravimetric data (¤).

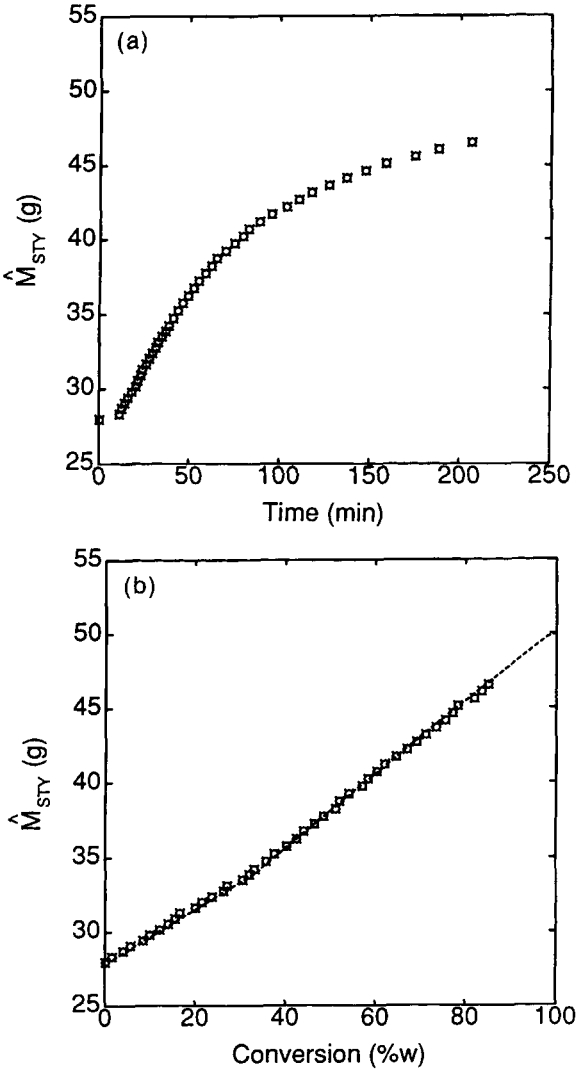

Figure 7 Amount of STY charged to the reactor in run 71 as a function of time (a) and conversion (b); experimental data (¤); calculated values (- - -).

The outcome of the composition-control monomer feed policy is illustrated in Figures 6–9. In this case, the composition-control problem is much less critical than for the previous system MMA–VAC. This conclusion is reflected by the similar kinetic behavior shown in Figure 6 in terms of conversion vs. time curves for the batch (run 65) and the semibatch (run 71) reactions. The amount of STY fed to the reactor is shown as a function of time in Figure 7(a) and as a function of conversion in Figure 7(b). The slope discontinuity, which occurs only in the second representation, corresponds to the discon-

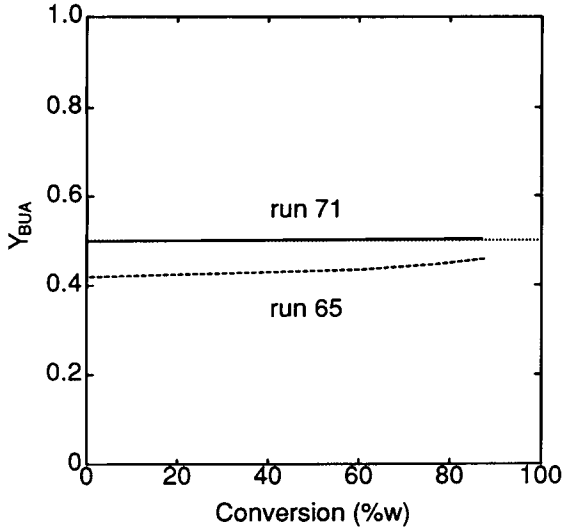

Figure 8 Calculated BUA weight fraction in copolymer, Y_{BUA} as a function of conversion; run 65 (- - -); run 71 (—); desired composition (· · ·).

tinuity in $\hat{Q}_{STY}$ arising at the transition from flooded to starved interval, i.e., at $M_c = M_c^*$.

The good performance of the composition-control monomer feed policy is illustrated in Figures 8 and 9, where the calculated compositions of the polymer, Y_{STY}, and of the overall monomer mixture in the reactor, Z_{STY}, respectively, are shown as a function of conversion. In Figure 9, the reliability of the calculated composition values is validated by comparison with the experimental values of monomer mixture composition measured by gas-chromatography. Note that this composition does not remain constant during the reaction. This is not surprising, and it does not indicate a poor composition control. This composition is not in fact the monomer composition in the reaction locus (i.e., in the polymer particles), but rather the overall composition in the reactor, which then reflects the variable buffering capacities of the various involved phases.

Ternary System MMA–VAC–BUA

To illustrate the application of the proposed polymer composition-control procedure to multicomponent systems, we consider next the ternary system methylmethacrylate–vinylacetate–butylacrylate (MMA–VAC–BUA). This system provides a significant test for the composition-control procedure, since the selected monomer species are characterized by different reactivities and water solubilities. In particular, three experiments are considered, one batch (run 72) and two semibatch reactions where the monomer species have been fed according to the optimal monomer feed policy (runs 74 and 80). The recipes adopted in each experimental run are summarized in Table II. In all cases, the objective is a polymer with constant composition: $Y_{VAC} = 0.40$, $Y_{MMA} = Y_{BUA} = 0.30$.

With reference to a final amount of polymer given by $M_c^f = 200$ g, the following monomer feed policy has been calculated:

	MMA	VAC	BUA
Y_i (−)	0.30	0.40	0.30
A_i (−)	8.65	0.54	9.98
B_i (g)	32.53	21.22	13.85
C_i (−)	0.042	0.920	0.038
$\hat{Q}_i^f$ (g/g)	0.281	0	0.284
$\hat{Q}_i^s$ (g/g)	0.284 ÷ 0.282	0	0.288 ÷ 0.285
$\hat{M}_i^0$ (g)	3.44	80.00	2.82

The copolymer amount corresponding to the transition from flooded to starved is $M_c^* = 25.8$ g. From the values of the parameter A reported above for the three monomers, we readily see that VAC is the critical monomer. Moreover, the values of the monomer flowrates do not change significantly during the polymerization reaction and actually remain rather close to the corresponding polymer composition, i.e., $\hat{Q}_{MMA} \simeq Y_{MMA}$ and $\hat{Q}_{BUA} \simeq Y_{BUA}$. This situation is similar to that encountered earlier in the case of the binary system MMA–VAC. In par-

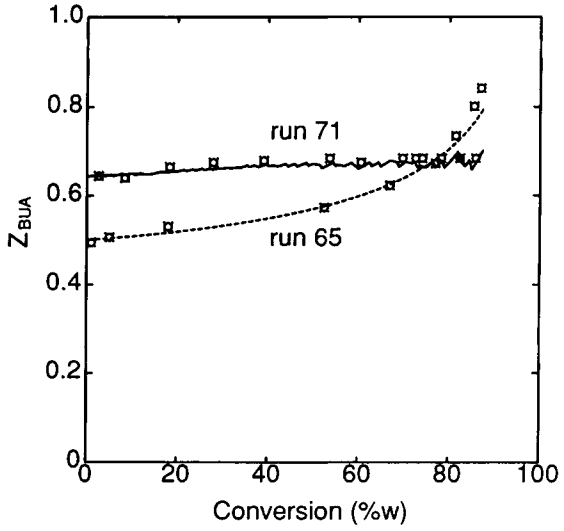

Figure 9 Overall composition of the monomer mixture in the reactor, Z_{BUA}, as a function of conversion for runs 65 and 71. Experimental data: (¤). Calculated curves: run 65 (- - -); run 71 (—).

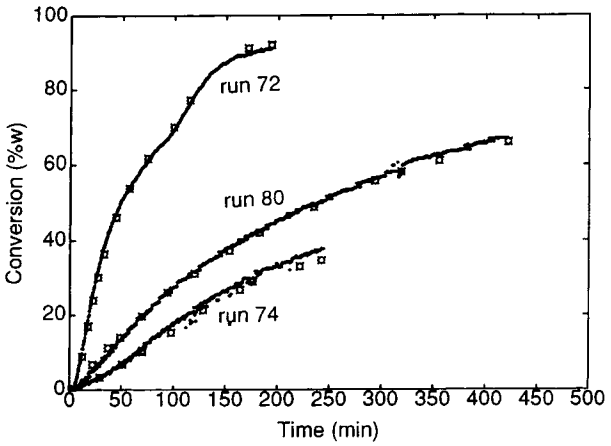

Figure 10 Conversion vs. time curves for runs 72, 74, and 80. Densimetric data (●); gravimetric data (¤).

ticular, since the value of A for the critical monomer is much lower than that for the other two monomers, we see from eq. (8) that $\hat{Q}f_{MMA} \simeq Y_{MMA}$ and $\hat{Q}f_{BUA} \simeq Y_{BUA}$. On the other hand, from eq. (15) we see that, since the water solubilities of the three monomers are not too different, the values of the monomer flowrates in the flooded and in the starved interval are rather similar.

The results of the experimental runs 72, 74, and 80 are shown in Figures 10–14. Let us first examine runs 72 and 74, i.e., two reactions with the same recipe but different procedure of monomer feeding, which were both stopped after about 4 h. The same comments previously reported with reference to the binary system MMA-VAC also applied to this case. From the conversion vs. time values shown in Figure 10, it was seen that the rate of polymerization was more uniform in the semibatch (run 74) than in the batch reaction (run 72), thus providing a qualitative indication of constant instantaneous polymer composition. Moreover, note that the on-line densimetric measurements are again in good agreement with the off-line gravimetric data.

The amounts of BUA and MMA added to the reactor according to the optimal feed policy are shown in Figures 11(a) and 12(a) as a function of time, and in Figures 11(b) and 12(b) as a function of conversion, respectively. The quality of the polymer produced is illustrated in Figures 13 and 14 in terms of the calculated compositions of the polymer, Y_i, and of the overall monomer mixture in the reactor, Z_i, respectively. In Figure 14, the calculated values are compared with the experimental data obtained by gas-chromatography. Also, in this case, data obtained for semibatch reactions are not very significant since, due to the very low reactivity of VAC, this monomer is always present in large excess, i.e., $C_{VAC} \simeq 1$.

Let us now proceed to consider the last experiment performed (run 80). This was again a semibatch reaction, performed under composition-controlled conditions. However, in this case a kinetic "disturbance" was deliberately introduced in the system. In particular, about 1 g $NaHCO_3$, usually adopted as buffering agent, was introduced in the reactor at the beginning of the reaction. The aim was to validate the insensitivity of the proposed composition-control procedure to recipe variations concerning those components affecting the polymerization rate without modifying the monomer

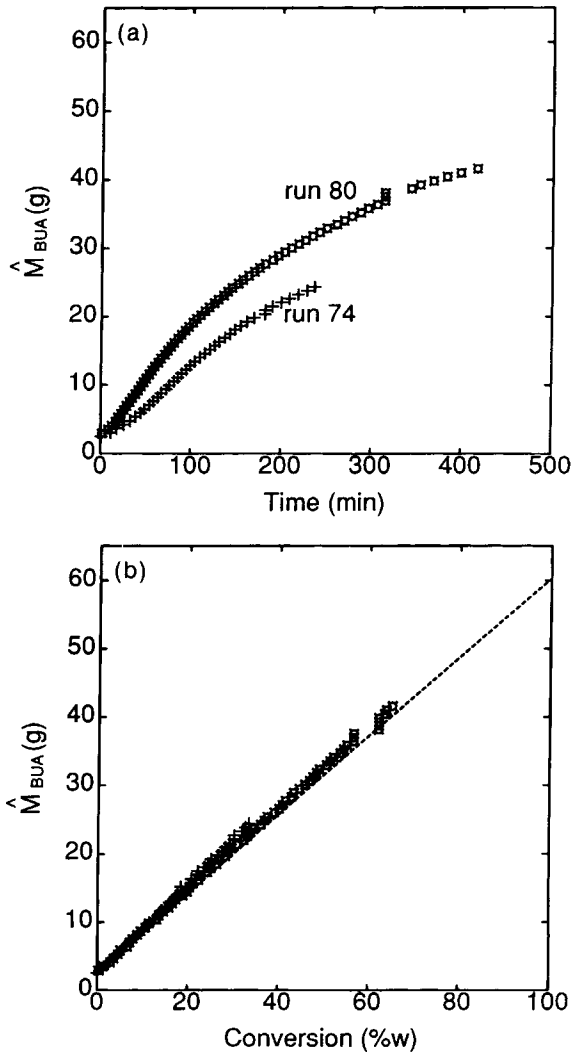

Figure 11 Amount of BUA charged to the reactor in runs 74 (+) and 80 (¤) as a function of time (a) and conversion (b); experimental data (+, ¤); calculated values (- - -).

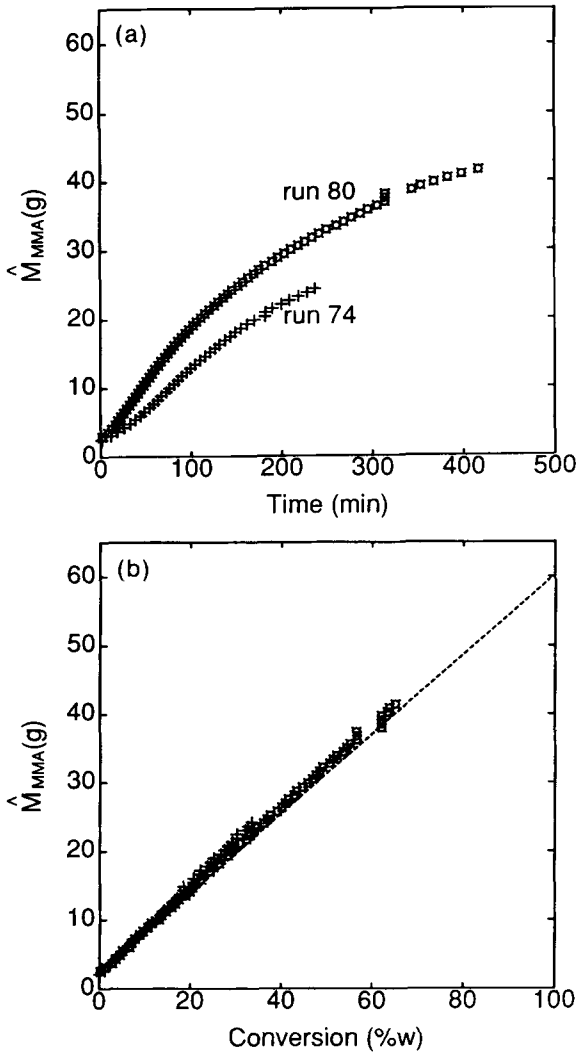

Figure 12 Amount of MMA charged to the reactor in runs 74 (+) and 80 (¤) as a function of time (a) and conversion (b); experimental data (+, ¤); calculated values (- - -).

partitioning, i.e., the composition evolution with respect to conversion. This was the case of the addition of $NaHCO_3$ which, as shown in Figure 10 (run 80), led to a significant increase in the rate of polymerization by affecting the nucleation stage. This was probably due to the effect of pH on the rate of decomposition of KPS. Note that this phenomenon was not accounted for by the model; however, it did not affect the reliability of the composition-control procedure, since the increased polymerization rate was detected by the on-line monitoring of conversion. As a result, we see from Figures 11 and 12 that the monomer feed policies for run 80 were different from those for run 74 when considered as a function

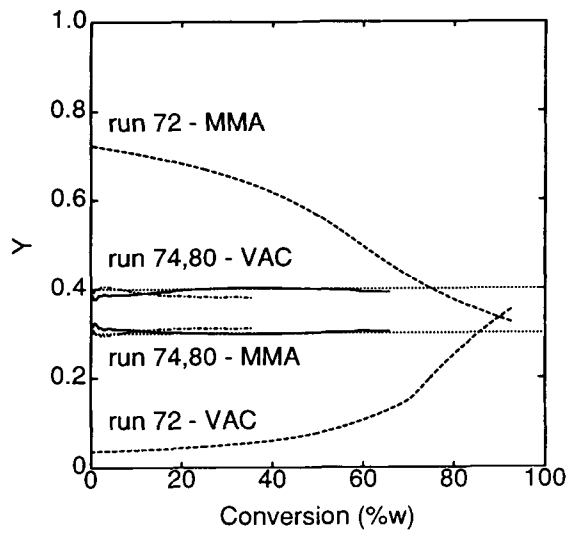

Figure 13 Calculated VAC and MMA weight fraction in copolymer as a function of conversion; run 72 (- - -), run 74 (- · - · -), and run 80 (—); desired composition (· · ·).

of time [Figs. 11(a) and 12(a)], while they became identical when considered as a function of conversion [Figs. 11(b) and 12(b)]. The quality of the composition control realized in run 80 is fully comparable to that obtained in run 74, as can be seen from the composition values shown in Figures 13 and 14.

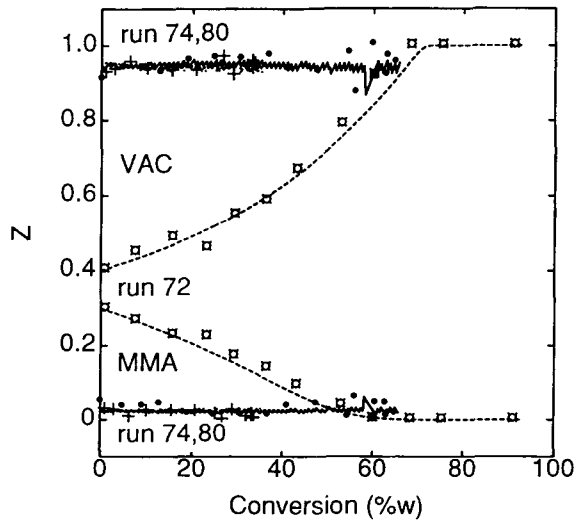

Figure 14 Overall compositions of the monomer mixture in the reactor, Z_{MMA} and Z_{VAC}, as a function of conversion. Experimental data: run 72 (¤); run 74 (+); run 80 (●). Calculated curves: run 72 (- - -), run 74 (- · · · -), and run 80 (—).

THERMAL CHARACTERIZATION

Direct characterization of the composition of the polymer produced has been performed through thermal analysis in the case of the MMA–VAC system discussed in the Binary System section. In particular, the thermal gravimetric analysis (TGA) has been applied to several samples corresponding to different conversion values, so as to follow the product characteristics as a function of conversion. On the other hand, only the final product has been analyzed by differential-scanning calorimetry (DSC).

The weight loss as a function of temperature, at fixed rate of temperature increase, as obtained by TGA, exhibits a characteristic pattern for each polymer. For example, in Figure 15 (a and b), the results of the TGA applied to the homopolymers of MMA and VAC, respectively, are shown. Let us now compare these results with those obtained by the TGA of the copolymers produced in this study. We expected these to be some sort of combination of the results corresponding to the pure monomer species shown in Figure 15 (a and b). The results of TGA of the copolymer samples prepared in the batch (run 56) and in the semibatch (run 62) reaction are shown for increasing conversion values Figure 15 (c and d) and in Figure 15 (e and f), respectively. Let us concentrate on the step increase of the weight loss in the low-temperature region, which is characteristic of the presence of VAC units in the polymer chains [see Fig. 15(b)]. In the case of the samples produced in the batch mode, we see that the entity of such a step increases with conversion [i.e., from Fig. 15(c) to (d)]. This indicates an increase of the VAC fraction in the polymer and then the presence of a compositional drift during the reaction. On the other hand, in Figure 15 (e and f), we see that, for the samples of polymer produced in the semibatch mode under composition-controlled conditions, the VAC content remains practically constant from low to high conversion values, which indicates a product of uniform composition.

The final polymer products have been analyzed by DSC to estimate the glass-transition temperatures, T_g. The measured T_g values of the homopolymers are in good agreement with those reported in the literature. The results obtained for the two copolymers (runs 56 and 62) are shown in Figure 16; in this case, we should recall that the T_g value is mainly related to the chain composition. Thus, when the instantaneous polymer composition remains constant during the entire polymerization process, we expect a single, well-defined glass transition, corresponding to a T_g value which depends on the specific composition of the copolymer. On the other hand, copolymer samples characterized by a broad composition distribution can be regarded as a mixture of copolymers with different T_g values, thus resulting in a DSC plot characterized by multiple, broad transitions. By inspection of Figure 16, it is possible to conclude that this is the case of the copolymer samples produced in the batch mode (run 56); two slope variations are present, thus indicating two values of T_g, the first one (29°C) very similar to that of VAC homopolymer and the second one, broadly distributed around 80°C, characteristic of a copolymer very rich in MMA. This result is due to the compositional drift during the reaction: at the beginning, a product very rich in MMA, the more reactive monomer, is produced; while an almost pure VAC homopolymer is produced in the last part of the reaction once MMA has been fully depleted. On the other hand, a single T_g value of 52°C characterizes the copolymer sample produced in the semibatch mode (run 62). This value agrees with that calculated from the T_g values of the pure homopolymers for a MMA–VAC copolymer with 70:30 weight composition and equal to 54°C.[13] Moreover, note that in this case the transition is very sharp, thus indicating a uniform product.

CONCLUSION

The theoretical optimal monomer feed policy for producing a polymer with constant instantaneous composition, in the minimum reaction time and with complete monomer depletion,[1] has been tested through the on-line measurement of conversion provided by a densitometer. The procedure has been applied to two binary and one ternary systems, thus confirming its capabilities with respect to multicomponent polymerizations. In all cases, a polymer with constant instantaneous composition along the entire reaction has been produced. Several characterization techniques have been used to support this conclusion. A rather important and unique aspect of the proposed approach is its insensitivity to time irreproducibilities, which are typical of these reacting systems and represent the major difficulty when implementing previously proposed composition-control policies based on some type of experimental iterative procedure.[14,15] In particular, this approach takes care of all irreproducibilities which affect the system behavior in terms of conversion vs. time, thus involving changes in the concentrations of emulsifier, initiator, or buffer agents. Irreproducibilities affecting the partitioning of the monomers in the var-

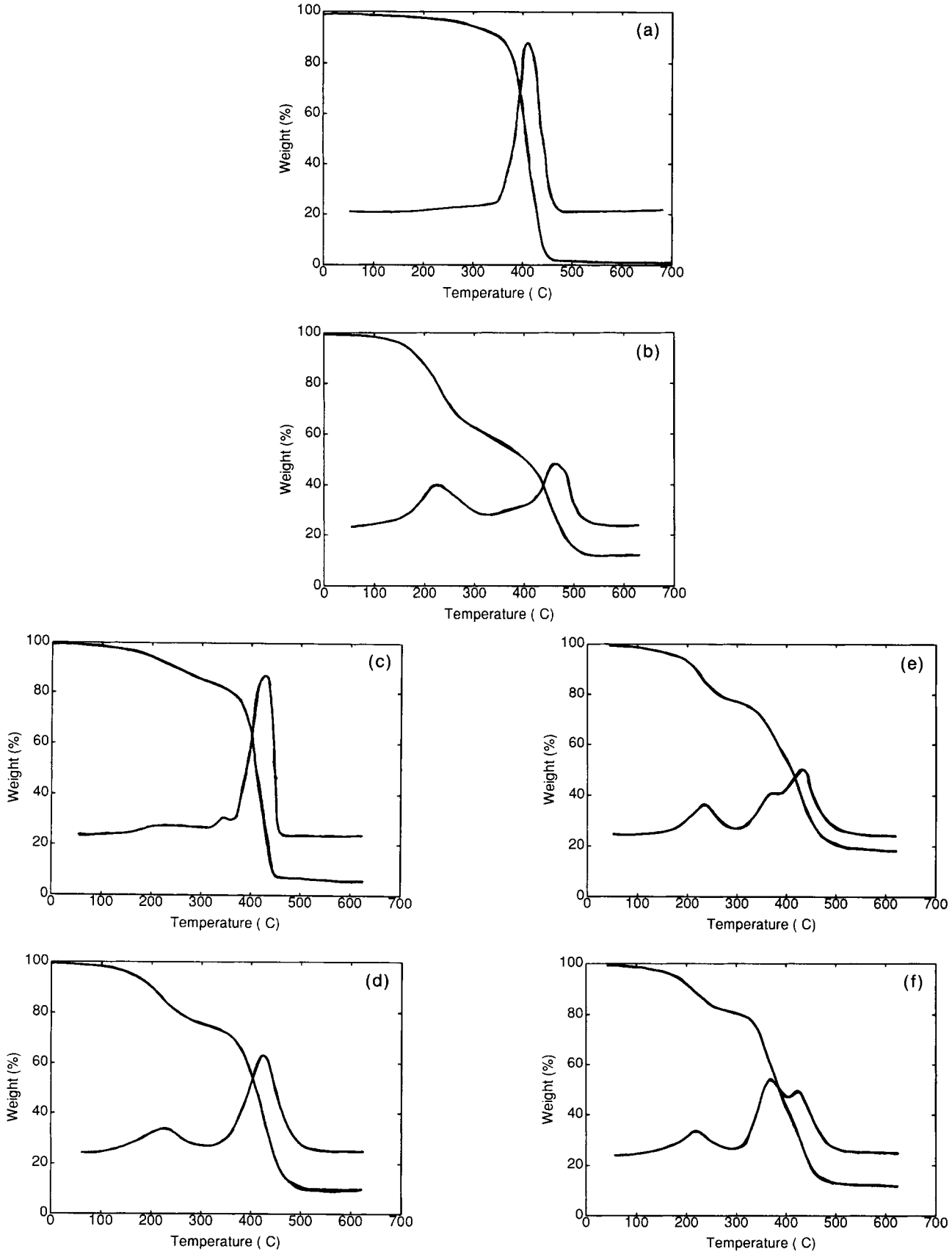

Figure 15 TGA results for MMA homopolymer (a), VAC homopolymer (b); MMA–VAC copolymer produced in the batch run 56 at low (c) and high (d) conversion; MMA–VAC copolymer produced in the semibatch run 62 at low (e) and high (f) conversion. Weight loss and derivative curves.

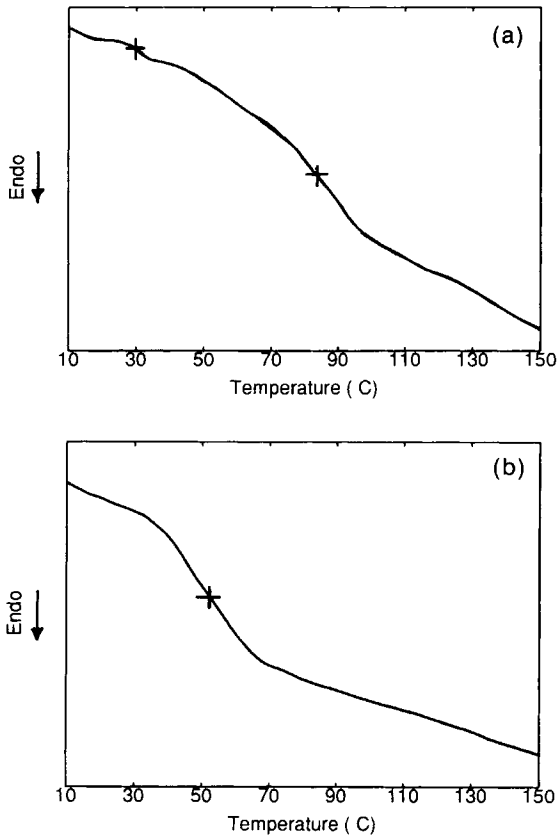

Figure 16 DSC results for final copolymer MMA–VAC produced in the batch run 56 (a) and final copolymer MMA–VAC produced in the semibatch run 62 (b).

ious phases or their intrinsic reactivities are not taken care of. It should be noted that in industrial applications, the first type of irreproducibilities is usually much more frequent.

The financial support by the Consiglio Nazionale delle Ricerche, Progetto Finalizzato Chimica Fine, is gratefully acknowledged.

NOMENCLATURE

A	densitometer calibration constant (g cm^{-3} s^{-2})
A_i	$= Y_i\rho_c/C_i\rho_i$
B	densitometer calibration constant (s^2)
B_i	$= M_i^{w,*}\rho_c/\phi^*\rho_i$ (g)
BUA	buthylacrylate
C_i	polymer-free volume fraction of monomer i in the polymer particles (ϕ_i/ϕ)
D_i	parameter defined by eq. (12)
M_c	overall amount of polymer produced in the reactor (g)
$\hat{M}_i$	total mass of monomer i charged to the reactor (g)
M_i^l	Amount of monomer i in phase l(g)
MMA	methylmethacrylate
MW_i	molecular weight of monomer i (g mol^{-1})
N_s	number of species
N_m	number of monomer species
KPS	potassium persulphate
$\hat{Q}_i$	massive feed flowrate of monomer i specific to the amount of polymer produced (g g^{-1})
r_{ik}	reactivity ratio ($= k_{pii}/k_{pik}$)
SLS	sodium lauryl sulphate
STY	styrene
T	period of oscillation (s)
T_g	glass transition temperature (°C)
VAC	vinylacetate
V_l	total volume of phase l (cm$_l^3$)
V_i^l	Volume of monomer i in phase l (cm$_l^3$)
v	specific volume (cm^3 g^{-1})
w	$M_c/(1-\phi)^2$
W_i	overall weight fraction of component i inside the reactor
y_i	mol fraction of monomer i in the polymer
Y_i	copolymer weight composition = $\frac{y_i MW_i}{\sum_j y_j MW_j}$
z	$= \phi/(1-\phi)$
Z_i	weight fraction of monomer i in the overall monomer mixture in the reactor

Greek Letters

ϕ_i	volume fraction of monomer i in the polymer particles
ϕ	volume fraction of monomers in the polymer particles ($= \sum_{i=1}^{Nm} \phi_i$)
ρ	density (g cm^{-3})
γ	parameter defined by eq. (10)

Subscripts

i	monomer species
j	critical monomer
c	copolymer
d	oil droplets
em	emulsion

Superscripts

f	final, flooded interval
s	starved interval
w	aqueous phase
0	initial
*	saturation

REFERENCES

1. P. Canu, S. Canegallo, G. Storti, and M. Morbidelli, *J. Appl. Polym. Sci.*, **54,** 1899 (1994).
2. R. G. Gilbert and D. H. Napper, *J. Macromol. Sci. Rev. Macromol. Chem. Phys.*, **C23,** 127 (1983).
3. J. M. Asua, M. E. Adams, and E. D. Sudol, *J. Applied Polym. Sci.*, **39,** 1183 (1990).
4. D. C. H. Chien and A. Penlidis, *JMS-Rev. Macromol. Chem. Phys.*, **C30,** 1 (1990).
5. F. J. Schork, *Continuous Monitoring of Emulsion Polymerization Systems*, E. P. I. 19th Annual Course, Lehigh Univ., Bethlehem, PA, 1988, Vol. 4.
6. F. J. Schork and W. H. Ray, *Am. Chem. Soc. Symp. Ser.*, **165,** 505 (1981).
7. S. Canegallo, G. Storti, M. Morbidelli, and S. Carra', *J. Appl. Polym. Sci.*, **47,** 961–979 (1993).
8. J. Brandrup and E. H. Immergut, *Polymer Handbook*, 3rd ed., Wiley, New York, 1989.
9. J. L. Gardon, *J. Polym. Sci.*, **6,** 2859 (1968).
10. F. R. Mayo and F. M. Lewis, *J. Am. Chem. Soc.*, **66,** 1594 (1944).
11. G. Storti, S. Canegallo, P. Canu, and M. Morbidelli, in *Polymer Reaction Engineering*, K. H. Reichert and H. U. Moritz, Eds., VCH, Weinheim, 1992, p. 379.
12. G. Storti, S. Carra', M. Morbidelli, and G. Vita, *J. Appl. Polym. Sci.*, **37,** 2443 (1989).
13. J. M. Barton, *J. Polym. Sci.*, **30,** 573 (1970).
14. G. H. J. Van Doremaele, H. A. S. Schoonbrood, J. Kurja, and A. L. German, *J. Appl. Polym. Sci.*, **45,** 957 (1992).
15. G. Arzamendi, J. C. De la Cal, and J. M. Asua, *Die Angewandte Makromolekulare Chemie*, **194,** 47 (1992).

Received February 21, 1994
Accepted June 8, 1994